

Characterization of TiAl intermetallic rods produced from elemental powders by hot extrusion reaction synthesis (HERS)

TIANYI CHENG

Metal Materials Section, Beijing Institute of Technology, Beijing 100081 and International Centre for Materials Physics, Academia Sinica, Shengyang 110012, People's Republic of China

M. McLEAN

Department of Materials, Imperial College of Science and Technology, Prince Consort Road, London SW7 2BP, UK

Rods of a mixture of two intermetallic phases, TiAl (γ) and Ti₃Al (α_2), have been produced directly from elemental powders of Ti–46.2 at% Al composition using a new hot extrusion reaction synthesis process (HERS) at a low initial temperature and over a short process time. The microstructures of the HERS rod were characterized by X-ray diffraction (XRD), optical microscopy, scanning electronic microscopy (SEM), transmission electronic microscopy (TEM) and energy dispersive spectroscopy (EDS). The microhardness of each phase was also measured. The dominant mechanisms during synthesis were analysed by combining these observations with the results obtained using differential scanning calorimeter (DSC).

1. Introduction

The intermetallic TiAl [1–3] has an attractive combination of properties including low density, relatively good oxidation resistance, high strength at room temperature and good creep behaviour at elevated temperature which makes it promising for high-temperature applications, particularly in the aerospace industry. However, TiAl is very brittle at room temperature due to its characteristic atomic bonding. Much recent work has concentrated on the improvement of the mechanical properties of TiAl for its proposed applications.

It is well known that careful control of the microstructures is a key factor in achieving good high temperature mechanical properties and acceptable room temperature ductility and toughness of TiAl. The most promising microstructure reported to date is a two-phase structure composed of γ and α_2 phases in alloys in the composition range of Ti–46 ~ 48 at% Al [1]. The usual process of ingot casting followed by thermomechanical processing such as isothermal forging has been used to produce the TiAl with the intended microstructures [4]. However, the high cost related to the slow cycle time, high processing temperatures and low product yield in this processing limits the possible use. In addition, the poor workability associated with the limited toughness and ductility remains a major barrier to producing semi-finished or final parts from TiAl.

Powder metallurgy provides an alternative route to producing TiAl intermetallics with two-phase microstructures. Canned hot forging and canned hot extrusion of alloy powder [4] are conventional processes which have been applied but the procedures are complex and involve very high process temperatures. Much attention has been focused on reaction synthesis processing starting from elemental powders to produce TiAl. It includes canned hot extrusion [5], cold extrusion [6] or cold rolling [7] followed by heat treatments. We have recently described a cost-effective process designated hot extrusion reaction synthesis (HERS) [8] and have applied HERS to produce Ni–Al alloys, Al–Ni–SiC and Al–Ti–SiC composites rods from elemental powders at relatively low initial temperatures over short process times. However, the content of intermetallics produced in these alloys and composites by HERS was estimated to be only about 5 vol% and a subsequent heat treatment is necessary to complete the reaction to produce a fully intermetallic structure.

This paper reports results of the further application of HERS processing to Ti–Al alloys. The attractive aspect of the work has been that two-phase microstructures of fully intermetallic γ and α_2 can be directly obtained by HERS at a low initial temperature and for a short process time. The microstructures of the HERS Ti–Al alloy have been characterized and the mechanisms controlling the formation of the microstructures are proposed.

2. Experimental procedure

Elemental commercial titanium powder with purity of 99.3% and an average size of $45\ \mu\text{m}$ and aluminium powders with an average size of $50\ \mu\text{m}$ produced by atomization at Imperial College were mixed prior to HERS processing. The major features of HERS processing have been described elsewhere [8]. The key point in HERS is that the extrusion temperature is only about one third of the melting temperature of the TiAl, which is considerably lower than that in traditional processing [4] and previously reported reaction synthesis processing [5]. The extrusion ratio in HERS is within the normal range of conventional hot extrusion processing [4, 5]. The microstructures of crosssections of the HERS Ti–Al alloy have been characterized by optical microscopy, scanning electron microscopy (SEM), transmission electron microscopy (TEM) and X-ray diffraction (XRD). Compositions of different phases in the Ti–Al rod have been determined using the analytical facilities of the JSM-35CF SEM with a minimum probe size of about $2\ \mu\text{m}$ and energy dispersive spectroscopy (EDS) in TEM. Using cobalt as a calibration element, an analysis error of $< 5\ \text{at}\%$ is achieved for most elements. Microhardness of each phase was measured using a load of 20 g. A mixture of powders with the same composition as the extruded rods was analysed by differential scanning calorimetry (DSC) using an argon atmosphere. The temperature range for the experiment was room temperature to 1200°C and heating and cooling rates were $20^\circ\text{C}\ \text{min}^{-1}$.

3. Results and discussion

A sound rod (Fig. 1) of the Ti–46.2 at% Al alloy with a length of about 1 m and a diameter of 14 mm was produced using HERS. No cracks were apparent on the rod surface although it dropped a distance of about 5 m on exiting the extrusion machine. The surface of the rod was generally smooth and very lightly oxidized, although the HERS was performed in air. This is due to the low processing temperature and the short extrusion time. The composition of the HERS processed rod determined by means of the conventional chemical analysis was confirmed to be Ti–46.2 at% Al.

Fig. 2 shows the microstructure imaged by optical microscopy. In addition to some porosity (shown as dark contrast and amounting to about 5 vol%) which is mainly distributed on grain boundaries, the microstructure consisted of two types of grains. The larger grains, which are about $25\ \mu\text{m}$ in diameter, have dark contrast and the smaller grains (about $10\ \mu\text{m}$) with light contrast. The microstructure is more clearly shown in the SEM micrographs in Fig. 3. The small grains have a polygonal morphology, suggesting occurrence of recrystallization. In the larger grains there is a fine precipitate (light contrast) which may lead to the dark contrast seen in optical microscopy because of diffraction effects. The precipitate particles are in the form of very small discontinuous rods aligned in the same orientation in each grain. In addition, an elongated block-like phase (white contrast) distributed mainly on grain boundaries.

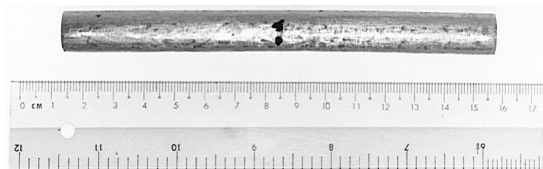


Figure 1 A piece of a sound Ti–46.2 at% Al rod, made using HERS processing.

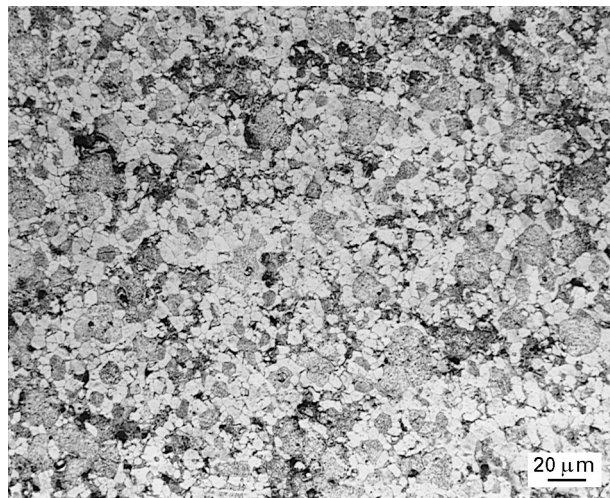


Figure 2 Optical micrograph of microstructures of HERS Ti–46.2 at% Al.

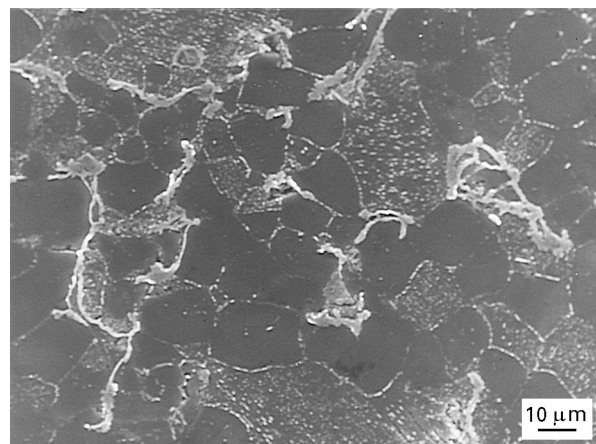


Figure 3 SEM micrograph of microstructures of HERS Ti–46.2 at% Al showing small grains, large grains containing precipitations and an elongated blocky phase on grain boundaries.

XRD analysis (Fig. 4) indicates that the HERS Ti–46.2 at% Al alloy only contains γ -TiAl and α_2 -Ti₃Al with no residual elemental aluminium or titanium, suggesting that the original aluminium and titanium has reacted completely during HERS within the analysis resolution of XRD. Based on the chemical analysis facility in SEM, the average compositions of small grains, large grains containing fine precipitation and block-like phases are estimated to be Ti–49.1 at% Al, Ti–40.4 at% Al and Ti–35.4 at% Al, respectively (Table I). Comparing these results with XRD analysis and the Ti–Al binary phase diagram [9] shown in Fig. 5, the small grains appear to be γ -TiAl and the

TABLE I Composition (at% Ti) of three areas in HERS Ti-46.2at% Al

Testing point	Small grain	Big grain	Block-like phase
1	50.5	59.9	64.6
2	50.7	59.4	68.2
3	51.4	59.5	64.1

elongated blocky phase to be α_2 -Ti₃Al. In the larger grain the matrix also is γ -TiAl and the fine precipitation is α -Ti₃Al. The microhardness of these three phases are 460 (TiAl), 810 (Ti₃Al) and 677 (TiAl + Ti₃Al precipitation), which is consistent with the above analysis since the α_2 with a DO₁₉ structure is harder and more brittle than γ with an ordered L1₀ structure.

TEM observation of microstructures of HERS Ti-46.2 at% Al (Fig. 6) shows similar features to those

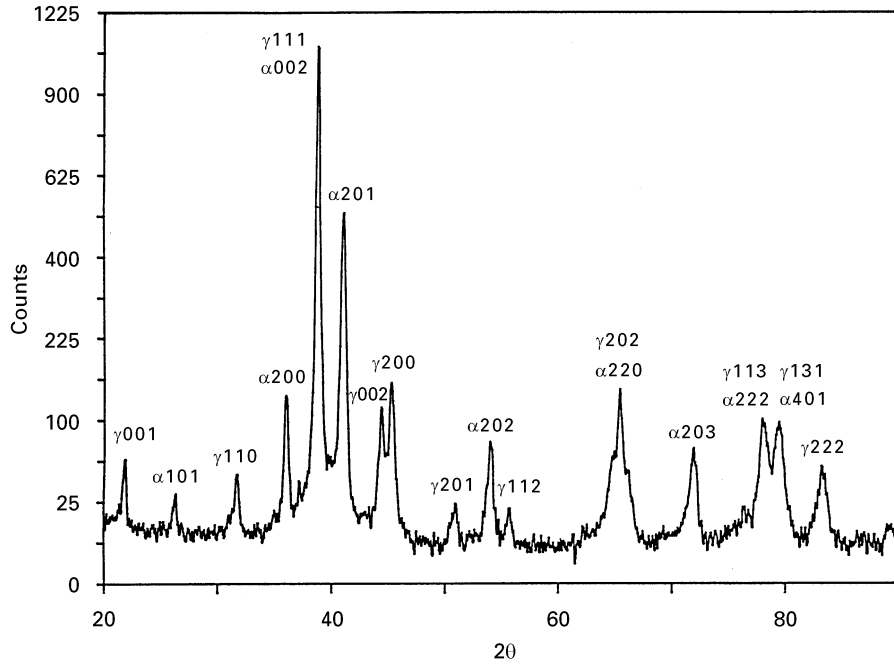


Figure 4 Indexed XRD pattern of HERS Ti-46.2 at% Al (γ : TiAl, α : Ti₃Al).

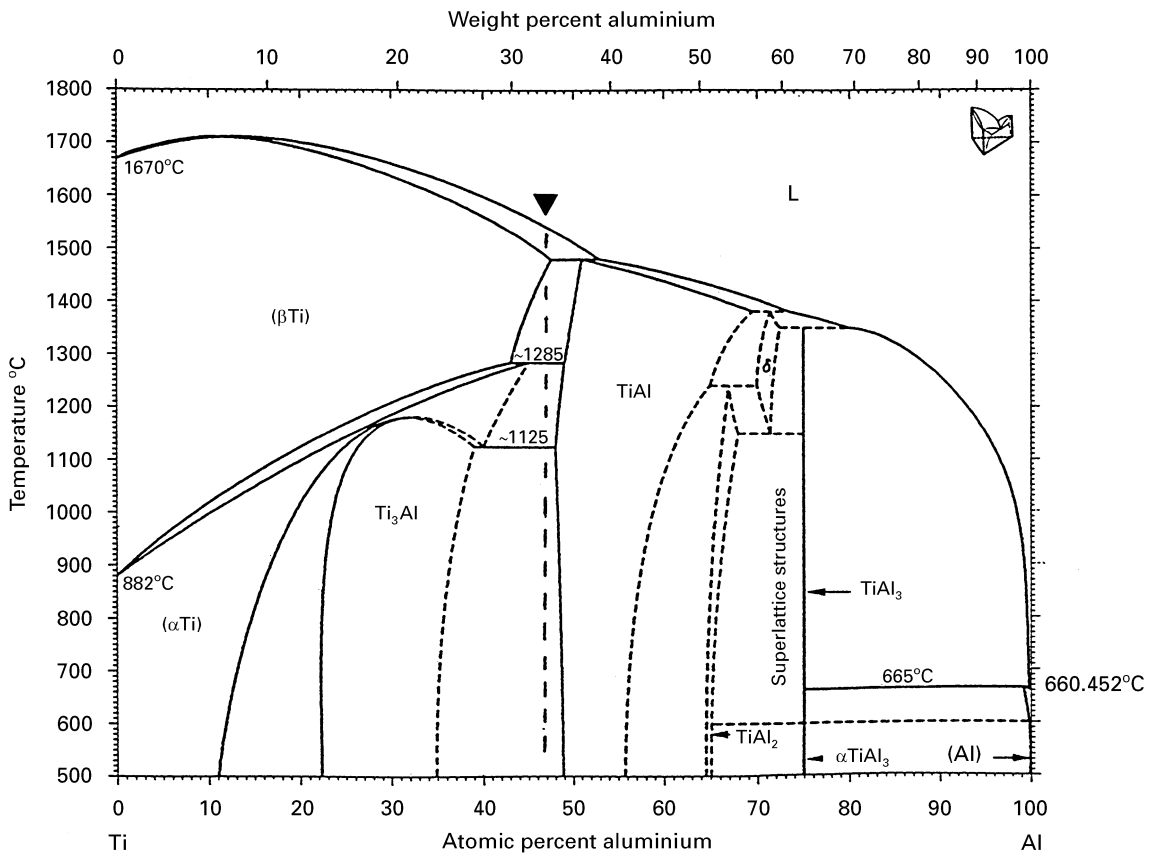


Figure 5 Ti-Al binary phase diagram [9] (the dash-plotted line indicates Ti-46.2 at% Al).

observed by SEM. A typical microstructure shown in Fig. 6a consists of small grains of γ (marked as I in the figure), a larger grain of γ containing many very fine precipitate particles of α_2 (II) and part of an elongated block-like particle of α_2 situated on grain boundaries (III). The result of EDS analysis in TEM is also consistent with the SEM chemical analysis. The average compositions of the three areas are determined to be Ti-51.3 at% Al (I), Ti-45.5 at% Al (III) and Ti-34.1 at% Al (II). Fig. 6b shows the EDS spectrum of γ and α_2 . The very fine α_2 precipitate with an average length of about 100 nm is shown in Fig. 6c. All precipitate particles have the same orientation and there is a strong interaction between precipitate particles and dislocations. There are some larger pre-

cipitate particles mainly in grains of type II. It is interesting to note that there is a fine precipitate-free-zone (PFZ) around the larger particles and along grain boundaries in area II. The EDS measurements indicate that the large precipitate particles are also α_2 and all of the PFZ are aluminium rich. These observations suggest that grain boundaries, at least in the area II, are titanium rich which is consistent with the elongated blocky α_2 being distributed mainly on the grain boundaries. In addition, many dislocations are concentrated around the interface between the larger α_2 particles and the γ matrix; this is probably associated with their different structures and thermal expansion coefficients. In some areas grains with lamellar structures can be seen (Fig. 7a).

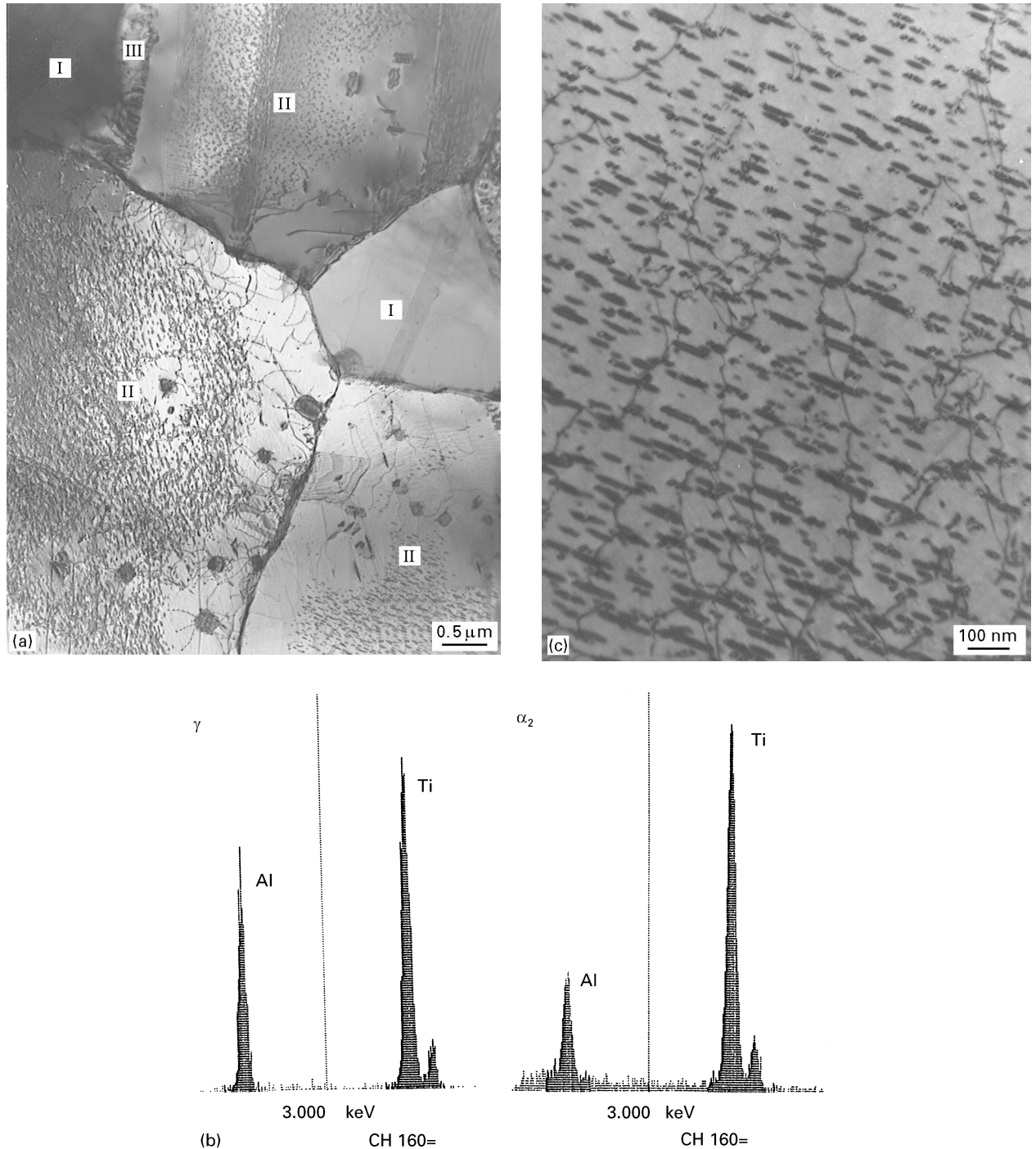


Figure 6 TEM micrographs of HERS Ti-46.2 at% Al showing: (a) small γ grain (I), larger γ grain containing α_2 precipitate (II) and elongated blocky α_2 on grain boundaries (III) (b) EDS spectra of γ and α_2 (c) fine α_2 precipitate.

These features are reminiscent of twinning but results of selected area electronic diffraction (SAED) and EDS measurements suggest that the lamella structure consists of alternate plates of γ and α_2 . Fig. 7b is a SAED pattern of γ plates (dark contrast) in the lamellar structure.

Fig. 8a shows a high density of dislocations in a γ grain (similar to area I in Fig. 6); although the TiAl

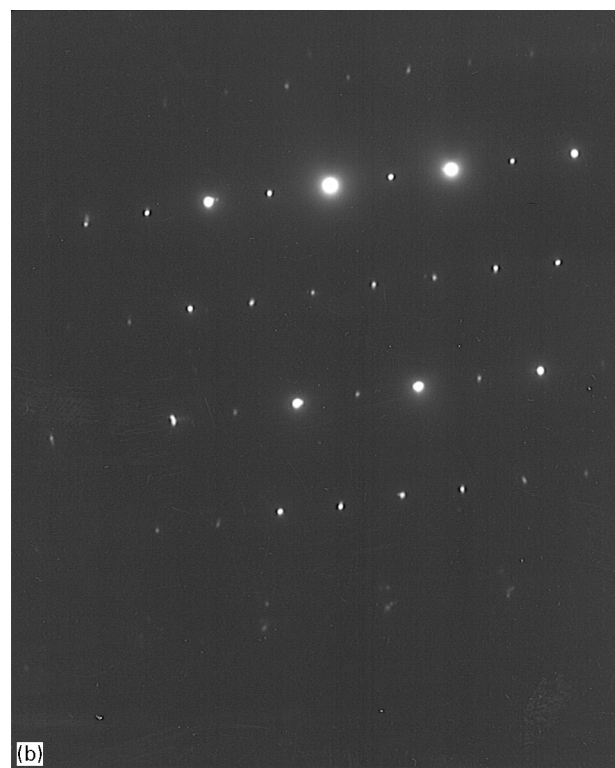
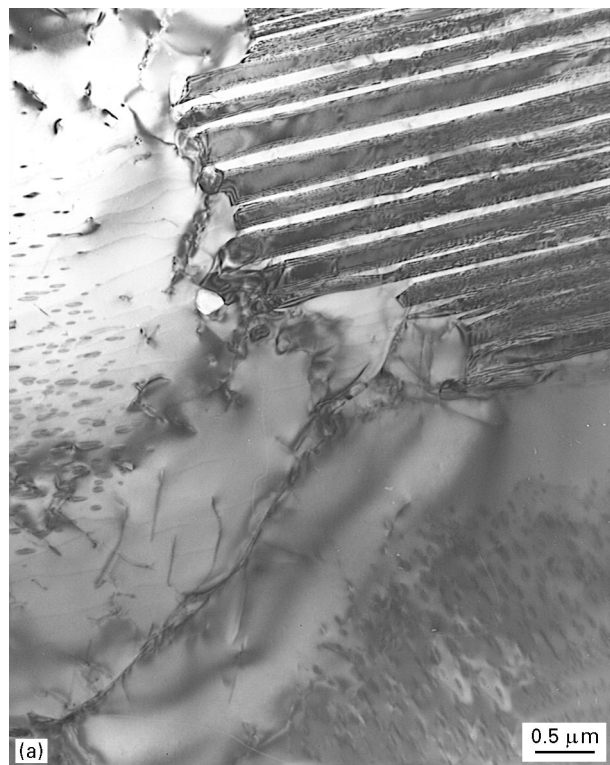


Figure 7 (a) Lamellar structure of γ and α_2 in a grain (top-right) and a γ grain containing α_2 precipitations (TEM micrograph); (b) SAED pattern of [1 1 3] zone of γ in the lamella structure.

alloy is intrinsically brittle, there are many dislocations in γ phase which are believed to result from extensive deformation in the later stage of HERS after the reaction and sintering are complete. It also relates to the relatively higher symmetry of the γ phase with a $L1_0$ structure compared with the $D0_{19}$ structure of α_2 . An interesting phenomenon shown in Fig. 8a and b is that some of the dislocations produced in the γ phase appear to be transmitted to the α_2 phase across the interphase boundaries. Deformation compatibility in neighbouring grains with different structures is an important reason for the transmission. A similar situation was observed in a two-phase NiAl–Ni₃Al alloy [10], in which the dislocations are transmitted from the relatively ductile Ni₃Al phase to brittle NiAl phase. This indicates the importance of maintaining an appropriate ratio of the γ phase to the α_2 phase in order to improve the room temperature brittleness of the two-phase Ti–Al alloy and to reach a balance between high temperature and room temperature properties.

The mechanism leading to the formation of microstructures of HERS alloys is an interesting issue. Fig. 9 shows DSC curves of the Ti–Al mixture during heating and cooling between room temperature and 1200 °C. It is apparent that there is an endothermic peak I and a large exothermic peak II during heating of a Ti–46.2 at% Al mixture of elemental powder; no peaks appeared during cooling. The relevant parameters of the two peaks are listed in Table II. The starting temperature of the reaction relevant to peak I is 652.7 °C, which is very close to the melting temperature of aluminium (660.4 °C), so it is probably related to partial melting of the aluminium powder as there was no evidence of melting on the surface of HERS rods. This peak actually consists of two endothermic peaks and the first being smaller. The reason for the peak splitting is not yet clear but may indicate that the melting of the aluminium powder occurs over a range of temperatures due to progressive aluminium diffusion into the titanium. A similar peak at 700 °C has been reported by Uneishi *et al.* [11] in elemental powder mixture of Ti–34 wt% Al but they did not report the exothermic peak. It is evident that melting of part of the aluminium powder will accelerate the diffusion and reaction between Al and Ti since the diffusion velocities of Al in Ti and Ti in Al in solid state at 648 °C are 0.075 $\mu\text{m s}^{-1}$ and 0.066 $\mu\text{m s}^{-1}$, respectively [12] but that of Ti in molten Al increases to 26 $\mu\text{m s}^{-1}$ [9], which is about 400 times higher than that in the solid state. Hence, the reaction between aluminium and titanium can proceed explosively at relatively low temperatures, which is similar to the self-propagating high-temperature synthesis (SHS) [8]. In fact, a much bigger exothermic peak (II) with a ΔH of 849.3 mJ mg^{-1} appeared in the DSC curve almost immediately following the endothermic peak (I), which should be a measure of the heat of reaction between elemental aluminium and titanium to form TiAl intermetallics. No separate peaks in the DSC curve are present corresponding to the formation of Ti₃Al and TiAl, respectively, probably because of the

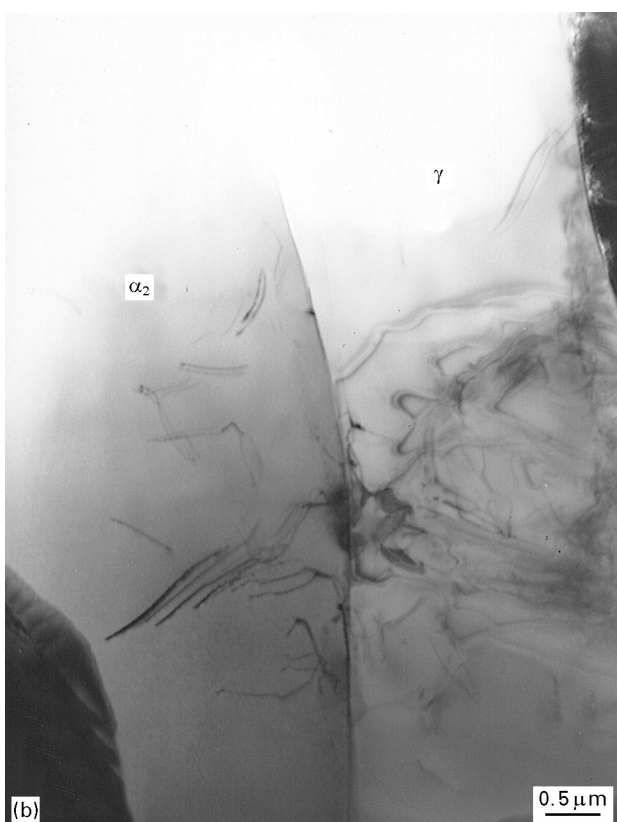


Figure 8 Dislocations in HERS Ti-46.2 at % Al (a) dislocations in γ grains; (b) dislocation transmission from γ to α_2 at a phase grain boundary (same area as (a)).

close proximity of their formation temperatures. The smaller Ti_3Al contents in the current alloy based on the Ti-Al phase diagram (Fig. 5) and the lower heat of formation of Ti_3Al (39 kJ mol^{-1}) than that of $TiAl$ (69 kJ mol^{-1}) [13] may also contribute to the super-

TABLE II Parameters of DSC curve of Ti-46.2 at % Al powder mixture

Peak	T_1 ($^{\circ}\text{C}$)	T_2 ($^{\circ}\text{C}$)	ΔH (mJ mg^{-1})
1	652.7	665.7	190.3
2	671.1	711.4	849.3

T_1 starting temperature of the reaction; T_2 peak temperature of the reaction, ΔH heat effects during the reaction.

position of these peaks. It is clear that the major heat production associated with the synthesis of TiAl intermetallics plays a key role in sintering and consolidation of the reacted intermetallics. The heat also facilitates hot extrusion of the normally brittle TiAl intermetallics to form the sound rod. In addition, the combination of the heat of reaction, the heat from internal and external friction during extrusion and the heat from the electric furnace in the hot extrusion facility provides the conditions for the kinetics of recovery and recrystallization of the intermetallics in the later stage of HERS although these may not be complete due to the limited time.

Based on the microstructures of HERS Ti-46.2 at % Al and above general analysis, it can be deduced that the two types of grains, Type I (smaller γ grains) and Type II (bigger γ grain with α_2 precipitation) are produced at different stages of the process. The smaller grains of TiAl form shortly after melting of part of the aluminium powder as the required composition is achieved by rapid liquid state diffusion. However, the TiAl formed will be aluminium rich compared with the average composition of the Ti-Al powder mixture based on the phase diagram (Fig. 5). The grain boundaries between this part of the reacted TiAl and the remaining elemental mixture i.e. the neighbouring area of the intermetallics first formed should be titanium rich. When the reaction continues in the remainder of the powder mixture with the help of the heat produced by the reaction in the first stage, the TiAl formed probably is non-equilibrium and titanium rich. The α_2 either precipitates in the larger grains or are formed on grain boundaries in the later stage but the lamellar structure of γ and α_2 can only form in parts of the grains because of the short time of the hot extrusion. Because of the early formation, the first part of the γ grains have time to recover and recrystallize so their grains are smaller than those in the second part of the TiAl formed. These deductions need to be further validated and the specific reactions in the process, including their effects on the texture of HERS rods and the reasons for the formation of different sizes (the fine and bigger) of α_2 precipitation, will be further studied.

Compared with conventional hot forging or hot extrusion processing the advantage of HERS is apparent in reducing the number of processing steps, thus saving energy and cost. The smaller reaction enthalpy between titanium and aluminium compared with that between nickel and aluminium is probably the major reason for the complete formation of TiAl

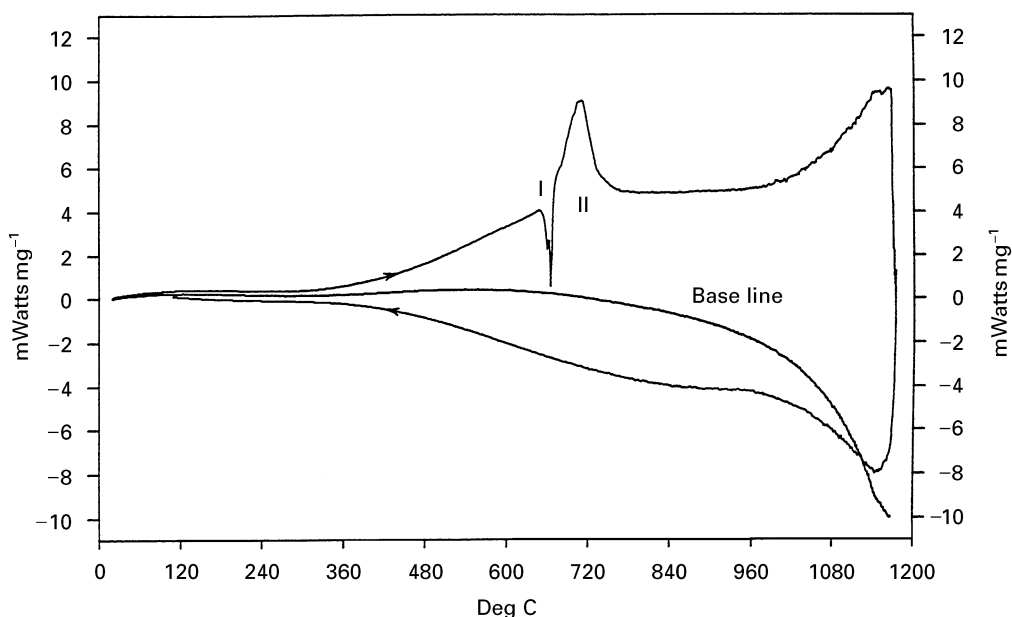


Figure 9 DSC curve of elemental powder mixture of Ti-46.2 at% Al during heating and cooling between room temperature and 1200 °C.

intermetallics during HERS. The major challenge for the application of the HERS processing is to identify a means of decreasing the porosity, which is mainly distributed on grain boundaries. Improvement of the processing parameters is a possible way to reach the goal.

4. Conclusions

1. Sound Ti-46.2 at% Al rods have been successfully produced by HERS processing at a relatively low temperature and for a short time. The rod consisted of fully intermetallic TiAl and Ti₃Al which were formed directly from elemental powders. Compared with conventional ingot casting followed by wrought processing HERS is a much simpler and cost-effective procedure. However, the porosity (about 5 vol%) is a major problem for the application of the process.

2. HERS-processed Ti-46.2 at% Al contains two types of γ -TiAl grains: small single-phase grains and larger grains containing a very fine α_2 -Ti₃Al precipitate. There is a PFZ along grain boundaries of the big grains and around the bigger precipitate particles. In addition, there is elongated blocky α_2 -Ti₃Al on some grain boundaries. The assumption about the formation process and the dominant mechanism of the microstructures have been presented.

Acknowledgements

The authors would like to thank the Royal Society for the financial support for the Joint Project.

References

1. Y. W. KIM, *J. Metals* **41** (1989) 24.
2. S.-C. HUANG and E. L. HALL, *Metall. Trans.* **22A** (1991) 427.
3. P. WANG, G. B. VISWANATHAN and V. K. VASUDEVAN, *ibid.* **23A** (1992) 690.
4. S. L. SEMIATIN, V. M. SEGAL, R. L. GOETZ, R. E. GOFORTH and T. HARTWIG, *Scripta Metall. Mater.* **33** (1995) 535.
5. I. S. LEE, S. K. HWANG, W. K. PARK, J. H. LEE, D. H. PARK, H. M. KIM and Y. T. LEE, *ibid.* **31** (1994) 57.
6. L. BATTEZZATI, C. ANTONIONE and F. FRACCHIA, *Intermetallics* **39** (1995) 67.
7. G. H. WANG and M. DAHMA, *Scripta Metall.* **26** (1992) 717.
8. TIANYI CHENG and M. McLEAN, *Mater. Lett.* **29** (1996) 91.
9. T. B. MASSALSKI, "Binary phase diagrams", (ASM, Metals Park, OH 1986) p. 175.
10. TIANYI CHENG, *J. Mater. Sci.* **30** (1995) 2877.
11. K. UENISHI, H. SUMI and K. F. K. OBAYASHI, *Z. Metallkde.* **86** (1995) 64.
12. J. POULIQUEN, S. OFFRET and J. DE FOUQUET, *C. R. Acad. Sci.* **C274** (1972) 1653.
13. K. SHIBUE, M. KIM and M. KUMAGAI, in Proceedings of the International Symposium on Intermetallic Compounds, JIMIS-6, edited by O. Izumi (JIM, Sendai, 1991).

Received 23 August 1996
and accepted 9 May 1997